Making anisotropy in seismic imaging models conformal with geology and velocity: application to standard tomographic and higher resolution FWI velocity modeling

Sergey Birdus, Alexey Artemov, and Li Li, CGG; Llew Vincent, Hess Exploration Australia*

Summary

In 2014 we proposed a new technique that used well information to correlate anisotropy with velocity for localized lithology dependent anomalies (Birdus *at al.*, 2014). It is based on the assumption that in appropriate geological settings localized variations in both velocity and anisotropy are caused by changes in the lithology. This results in some correlation between anisotropy and velocity anomalies. We used well information to establish such a correlation for tomographic PSDM imaging anisotropic velocity models. In this paper we extend our approach to high resolution FWI depth velocity modeling. We use a real 3D seismic dataset from the NW Australian shelf to illustrate how our technique produces more realistic anisotropic velocity models and reduces depth misties.

Introduction

Having an accurate anisotropy model is very important for depth-velocity modeling, in particular for correct positioning of seismic reflectors in depth. The effective seismic velocity V_seis (seismic moveout) in VTI media depends on the true vertical velocity V_vert and anisotropic parameter δ (Thomsen, 2002):

$$V\_seis = V\_vert * \sqrt{1+2\delta} \qquad (1)$$

The same effect is present in more complex models for anisotropy (TTI, orthorhombic etc). If we use only seismic data we are not able to separate the two factors in the right hand side of equation (1), i.e., we cannot unambiguously distinguish arrival time variations due to velocity and anisotropy. This leads to uncertainties in velocity/anisotropy estimations. In this paper, we focus on the elliptical component of anisotropy (δ = ε), which is responsible for the errors in depth estimation. We concentrate on small and medium-size anomalies when the major global trends are known.

Uncertainties and depth misties in anisotropic depth-velocity modelling and imaging.

We use seismic data, available well information and a-priori geological knowledge to build imaging anisotropic depth-velocity models. The problem with uncertainties is resolved by creating the simplest model that satisfies all input data (Artemov and Birdus, 2014). Traditionally we put all detected small scale anomalies into the imaging velocities and set the anisotropy values using simplified smoothed models.

For the well locations, depth misties after depth-velocity modeling and imaging can be estimated by two methods: (a) compare seismic events on images in depth with corresponding geological well markers or (b) compare check-shot based time-depth pairs with time-depth curves calculated for our velocity models.

In general, two approaches can be used to reduce observed depth misties. We refer to the first as “standard well calibration”. In this approach, we (1) locally compare seismic velocities to the well data, (2) calculate vertical profiles of anisotropic parameter δ for the well locations that would remove the misties and preserve seismic moveout, (3) interpolate δ values between the wells and (4) create calibrated velocity and anisotropy volumes. In this way, we can get zero (or significantly reduced) depth misties for the existing well locations and keep residual moveout unchanged. Such calibration has limited value as it is prone to the “bull’s eye” effect, often cannot be explained geologically, does not guarantee reliable depth estimation for future well locations and can make subsequent well-based uncertainty analysis difficult.

The second approach is based on the idea that existing depth errors/misties are primarily caused by the velocity-anisotropy uncertainty. They can be reduced if we solve this uncertainty by using additional information. Duranti (2010) and Bachrach (2010) proposed similar models to tie anisotropy with velocity for shales as a function of the compaction load. These models describe global compaction driven trends that can be observed in many parts of the world: anisotropy increases in line with velocity within the shallow part of the model, reaches its maximum value at depth around 500-800m below the sea floor and can decrease at much deeper intervals. Localized lateral velocity and anisotropy anomalies cannot be described by this “shale compaction” model because they are caused by changes in the lithology (shale vs carbonate vs sandstone etc) happening at the same depth. Our proposed technique uses well information to find anisotropy-velocity correlation for such localized lithology dependent anomalies. If this correlation is observed we can use it to build more accurate and geology consistent models for δ.

Application in anisotropic tomographic modeling

We illustrate the proposed workflow on a 2300 sq km 3D marine dataset from the North-West Australian shelf. Figure 1 shows the initial isotropic interval velocity model created from Vrms and the corresponding PSDM image.

DOI http://dx.doi.org/10.1190/segam2015-5831251.1

Depth misties (blue dots on Figure 1c) were estimated by comparing 2 target horizons on the PSDM volume (depth interval 2.5-3.0 km) with geological markers in 8 wells. All the misties were positive. This meant that the initial isotropic imaging velocities were too high.

Blue lines on Figure 2a are vertical profiles of the initial velocity at the well locations. Blue lines on Figure 2a are depth misties estimated by comparing available check-shot time-depth curves with time-depth values calculated for the initial velocity model at the well locations. At target level, these misties are similar to the misties based on geological markers (blue dots on Figure 1c).

Our standard 3D anisotropic tomographic depth-velocity modelling produced the result shown on Figures 3a,b,c (also see green lines on Figure 2). The velocity model (Figure 3a) now includes significant localized velocity variations mainly associated with layers of high velocity carbonates within relatively low velocity shales. Anisotropy model (Figure 3b and green lines on Figure 2b) followed the generalized shales compaction trend. Anisotropy values were tied to the sea floor horizon without any lateral variations except for a decrease at the major regional unconformity. Anisotropy values were calculated to minimize the depth misties and satisfy a-priori geological expectations.

As we can see on Figures 2c and 3c, this standard anisotropic velocity modelling removed the global trend in depth misties. Now all misties are centred around zero with the standard deviation decreased from 34.6 m (the initial model) to 12.6 m. Observed variations between minimal and maximal misties were reduced from 104 m to 35 m. These numbers demonstrate how our standard depth-velocity modelling reduced the structural depth uncertainty.

We could further reduce existing depth misties by applying standard well calibration as described in the previous section. Instead we investigated if we could create a geologically conformal model for anisotropy and reduce the depth misties (uncertainty in our depth estimations) in a geologically meaningful and controllable way.

The current anisotropy model (Figure 3b) is much simpler than the velocity field (Figure 3a). It is because we transformed localized variations in seismic moveout entirely into localized velocity anomalies. This was our standard solution to the velocity-anisotropy uncertainty problem but in this case it was not the most realistic.

Localized velocity variations correspond to changes in lithology. We can assume that these changes in lithology also create some variations in anisotropy, in which case we need to find a way to quantify such anisotropy anomalies.

As the changes in both velocity and anisotropy are caused by the lithology we can assume that there should be a correlation between localized variations in velocity and localized variations in anisotropy: $\delta\_var \sim V\_var$. If we use the simplest and robust linear correlation, we get the following equation to tie variations in anisotropy and velocity: $\delta\_var = \boldsymbol{S} * V\_var$ or

$$\delta(X,Y,Z) - \delta\_trend(X,Y,Z) = \boldsymbol{S} * (V(X,Y,Z) - V\_trend(X,Y,Z)). \quad (2)$$

δ_trend and V_trend are smoothed functions similar to what we see on Figures 1a and 3b. ***S*** is the correlation ratio, which can be set as a constant for a certain interval. For any given value of ***S***, we change anisotropy using equation (2). At the same time we honour the seismic data and preserve the moveout (V_seis) by changing the vertical velocity accordingly to satisfy equation (1). The updated vertical velocity automatically changes all well based depth misties. Applying the above sequence, we transform localized seismic moveout anomalies into localized anomalies in both vertical velocities and anisotropy. The value of ***S*** determines how much goes into the anisotropy. Our objective is to find an optimal value for ***S*** that minimizes the standard deviation of the misties. We use the standard deviation because this parameter describes the uncertainty of our depth estimations and this is what we want to reduce. Skipping some computational details we show our results on Figures 3d,e,f and 4.

The anisotropy (Figure 3e) is now conformal with velocity and geology. Both anisotropy and vertical velocity values have been changed by few per cent (from green to red lines on Figure 2). As a consequence, the events on the seismic image moved vertically by up to plus/minus 10 m. All this significantly reduced the depth misties (the standard deviation decreased from 12.6 m to 5.8 m and the variations between minimal and maximal values from 35 m to 19 m).

As a result, we created an effective imaging anisotropy model δ(X,Y,Z) that is similar to the imaging velocities: it produces flat PSDM gathers, best focused image and minimal depth misties. The localized anisotropy anomalies are caused by real intrinsic anisotropy and quasi-anisotropy due to thin layering effects. If needed, after building a geologically conformal anisotropy model, the requirements of conformity can be relaxed to apply a more standard well calibration sequence for the smaller remaining misties and with smaller possible negative side effects.

Our correlation analysis requires a sufficient number of wells crossing geological objects with different velocity/anisotropy values. This condition was met on our project. Figure 4 shows a 3D view of the final model with

DOI http://dx.doi.org/10.1190/segam2015-5831251.1

the well locations and the horizontal slices at the level of the strongest lateral velocity/anisotropy variations. Working within the same geological province, we gain experience after each project with wells and this experience (the velocity/anisotropy correlation coefficients) can be applied to new areas with limited or without any well information.

Application to high resolution FWI velocity modeling

High resolution FWI velocity modelling in anisotropic media faces the same uncertainty between vertical and inverted FWI velocities. FWI mainly depends on seismic events travelling in quasi-horizontal directions with little influence on δ or vertical velocity (Plessix and Cao, 2011; Alkhalifah, 2014). The problem can be solved under our elliptical anisotropy assumption by using correlation between δ and velocity (either measured on FWI results if a sufficient number of wells is available or derived using tomography). Figure 5 shows an example: FWI velocity modelling improved resolution, added new details and resolved some structural distortions (Figure 5c vs Figure 5a). If we keep the δ field without update (as Figure 5b) the depth will not be accurate. In our case we used anisotropy/velocity correlation parameters measured in nearby 3D tomographic PSDM project to produce a more geological high resolution δ model (Figure 5d) that corrected depth misties associated with the anisotropy.

Conclusions

Making anisotropy conformal with velocity and geology in appropriate geological settings results in more accurate and realistic anisotropic velocity models. It reduces depth misties and overcomes the negative side effects of the standard well calibration. In our case we observed strong correlation between δ and velocity for intervals consisting of high velocity carbonates and low velocity shales.

Acknowledgments

We thank Hess Exploration Australia and CGG for permission to present these results.

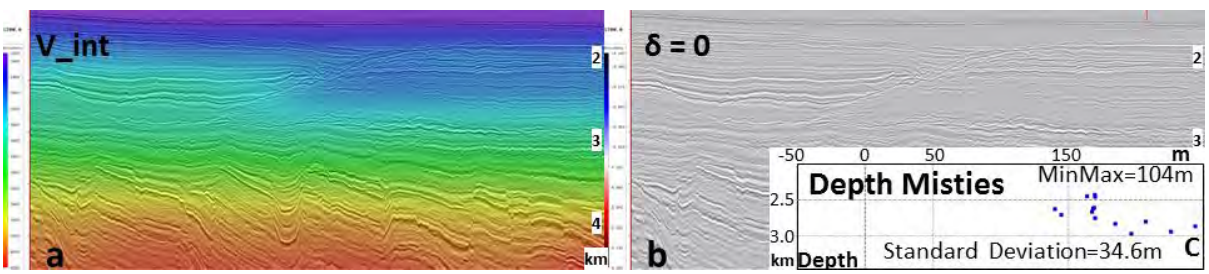

Figure 1. (a) and (b) Initial isotropic velocity model and corresponding PSDM image; (c) seismic to well markers depth misties.

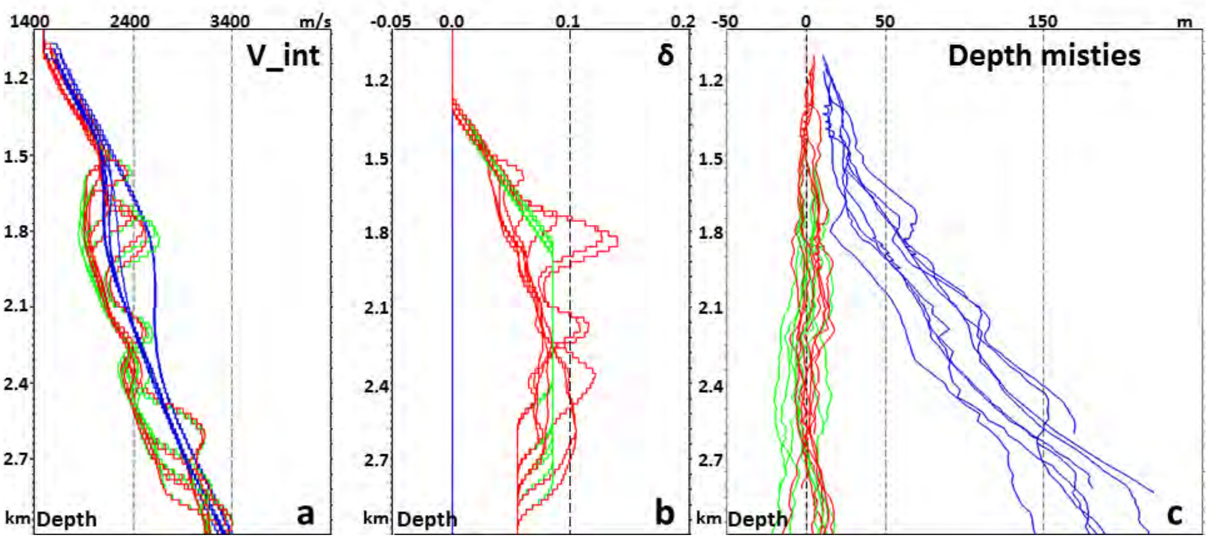

Figure 2. (a) Interval velocity profiles for 8 available well locations; (b) Anisotropic parameter δ; (c) Checkshot based depth misties. Blue: initial isotropic model. Green: model after standard anisotropic tomography. Red: model with anisotropy conformal to geology.

DOI http://dx.doi.org/10.1190/segam2015-5831251.1

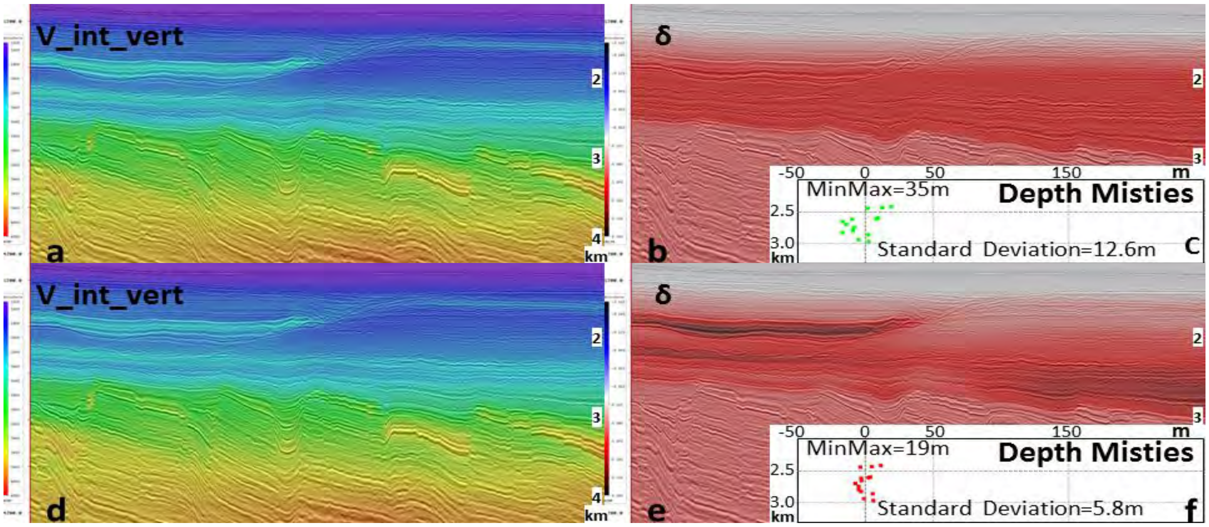

Figure 3. (a,b,c) Model after standard anisotropic tomography and (d,e,f) model with anisotropy conformal to geology.

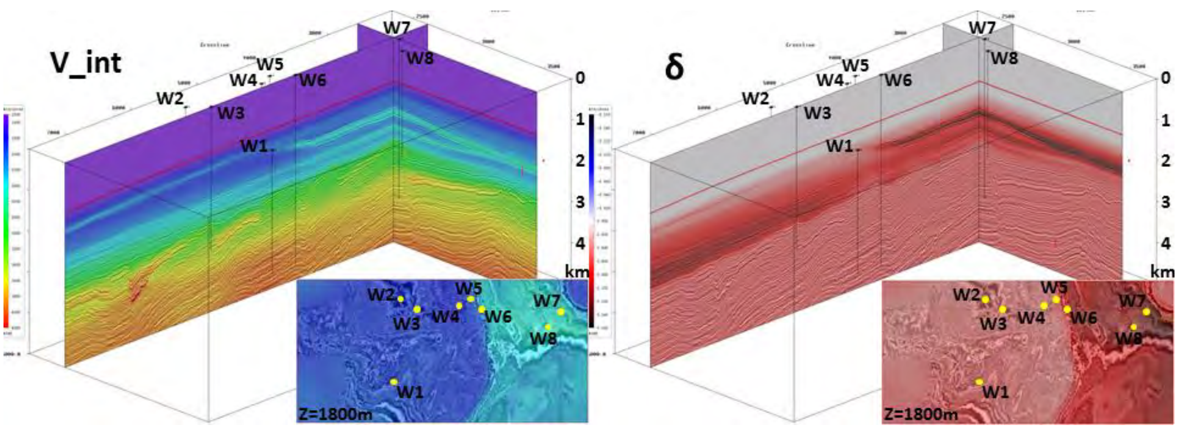

Figure 4. 3D view of the final model with the well locations.

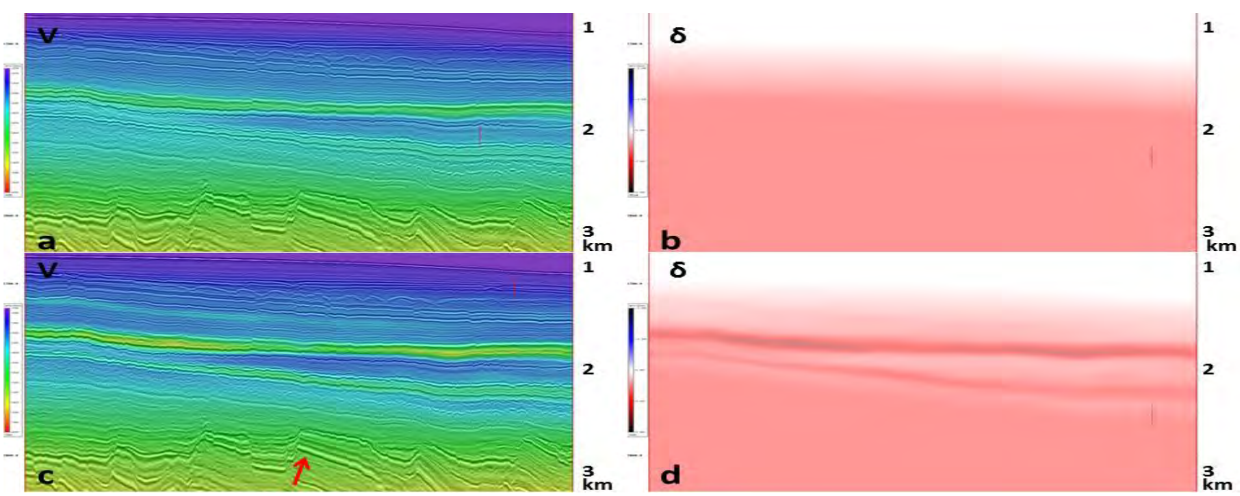

Figure 5. (a,b) Model after standard tomographic model building; (c,d) model after FWI with anisotropy conformal to geology.

DOI http://dx.doi.org/10.1190/segam2015-5831251.1

EDITED REFERENCES

Note: This reference list is a copyedited version of the reference list submitted by the author. Reference lists for the 2015 SEG Technical Program Expanded Abstracts have been copyedited so that references provided with the online metadata for each paper will achieve a high degree of linking to cited sources that appear on the Web.

REFERENCES

Artemov, A., and S. Birdus, 2014, Reducing geologically significant structural uncertainties in anisotropic depth-velocity modeling in settings typical for the North-West Australian shelf: 84th Annual International Meeting, SEG, Expanded Abstracts, 306–310.

Alkhalifah T.A., 2014, Full-waveform inversion in an anisotropic world: Where are the parameters hiding?: EAGE.

Bachrach, R., 2010, Applications of deterministic and stochastic rock physics modeling to anisotropic velocity model building: 80th Annual International Meeting, SEG, Expanded Abstracts, 2436–2440.

Birdus, S., L. Vincent, R. Djumeno, A. Artemov, and L. Li, 2014, Reducing depth misties by making anisotropy conformal with velocity and geology — Example from the NW Australian Shelf: 76th Annual International Conference and Exhibition, EAGE, Extended Abstracts, Tu P02 04.

Duranti, L., 2010, On the constitutive equation of elastic anisotropy of shales: EAGE Shale Workshop, Workshop proceedings, C01.

Plessix, R., and Q. Cao, 2011, A parametrization study for surface seismic full-waveform inversion in an acoustic vertical transversely isotropic medium: Geophysical Journal International, **185**, no. 1, 539–556. http://dx.doi.org/10.1111/j.1365-246X.2011.04957.x.

Thomsen, L., 2002, Understanding seismic anisotropy in exploration and exploitation: SEG. http://dx.doi.org/10.1190/1.9781560801986.

DOI http://dx.doi.org/10.1190/segam2015-5831251.1